A dense brown trout (*Salmo trutta*) linkage map reveals recent chromosomal rearrangements in the *Salmo* genus and the impact of selection on linked neutral diversity

Maeva LEITWEIN[*], Bruno GUINAND[*†], Juliette POUZADOUX[*], Erick DESMARAIS[*], Patrick BERREBI[*], Pierre-Alexandre GAGNAIRE[*‡]

Addresses :

[*]: UMR ISEM, Institut des Sciences de l'Evolution de Montpellier, Université de Montpellier, Place E. Bataillon - cc65, 34095 Montpellier Cedex 5, France

†: Département Biologie-Ecologie, Université de Montpellier, Place Eugène Bataillon, 34095 Montpellier Cedex 5, France

‡: Station Biologique Marine, 2 Avenue des Chantiers, 34200 Sète, France

15 Running title: A dense *Salmo trutta* linkage map

16 Key words: Linkage mapping, *Salmo trutta*, Salmonids, RAD markers, Recombination rate

17

18 Corresponding Author:

19

20 Maeva Leitwein

21 ISEM-Institut des Sciences de l'Evolution

22 UMR5554

23 C.C. 065

24 Place Eugène Bataillon –

25 Université Montpellier

26 34095 Montpellier cedex 05

27 France

28 Tel.: +33 467143725;

29 email: maeva.leitwein@umontpellier.fr

30

ABSTRACT

High-density linkage maps are valuable tools for conservation and eco-evolutionary issues. In salmonids, a complex rediploidization process consecutive to an ancient whole genome duplication event makes linkage maps of prime importance for investigating the evolutionary history of chromosome rearrangements. Here, we developed a high-density consensus linkage map for the brown trout (*Salmo trutta*), a socio-economically important species heavily impacted by human activities. A total of 3,977 ddRAD markers were mapped and ordered in 40 linkage groups using sex- and lineage-averaged recombination distances obtained from two family crosses. Performing map comparison between *S. trutta* and its sister species *Salmo salar* revealed extensive chromosomal rearrangements. Strikingly, all of the fusion and fission events that occurred after the *S. salar*/*S. trutta* speciation happened in the Atlantic salmon branch, whereas the brown trout remained closer to the ancestral chromosome structure. Using the strongly conserved synteny within chromosome arms, we aligned the brown trout linkage map to the Atlantic salmon genome sequence to estimate the local recombination rate in *S. trutta* at 3,721 loci. A significant positive correlation between recombination rate and within-population nucleotide diversity (π) was found, indicating that selection constrains variation at linked neutral sites in brown trout. This new high density linkage map provides a useful genomic resource for future aquaculture, conservation and eco-evolutionary studies in brown trout.

INTRODUCTION

A renewed interest for linkage mapping studies has recently occurred thanks to the simplified procedures for generating large genotype datasets in non-model organisms (Slate *et al.* 2008; Stapley *et al.* 2010; Ekblom and Galindo 2011). High-density linkage maps have been particularly developed in teleost fishes, because of their high number of species, their economic importance for aquaculture (e.g., Sauvage *et al.* 2012; Zhao *et al.* 2013; Wang *et al.* 2015; Liu *et al.* 2016; Kumar and Kocour 2017), their phylogenetic position within vertebrates (Amores *et al.* 2011; Rondeau *et al.* 2014; Wang *et al.* 2015; Kuang *et al.* 2016), as well as their broad interests for eco-evolutionary and conservation/management issues (Everett *et al.* 2012; Gagnaire *et al.* 2013a; Kai *et al.* 2014).

The salmonid family, which has 11 genera and more than 60 species (Crête-Lafrenière *et al.* 2012), is a group of fish in which numerous initiatives have been developed to construct high-density linkage maps (Brieuc *et al.* 2014; Gonen *et al.* 2014; Limborg *et al.* 2015b; Larson *et al.* 2016; Tsai *et al.* 2016). Besides their applications for mapping traits of importance for aquaculture (Houston *et al.* 2012; Sauvage *et al.* 2012; Tsai *et al.* 2015), salmonid linkage maps have catalysed molecular ecology and genome evolution studies over the last recent years. Several studies have used linkage map information for addressing eco-evolutionary and related conservation biology issues at the species level or among hybridizing taxa (Lamaze *et al.* 2012; Bourret *et al.* 2013; Perrier *et al.* 2013; Gagnaire *et al.* 2013b; Limborg *et al.* 2014; McKinney *et al.* 2015). A second category of studies have focused on understanding the evolutionary consequences of the whole genome duplication event (salmonid-specific fourth vertebrate whole genome duplication; WGD-Ss4R) that occurred within the salmonid family around 60 Mya ago (Crête-Lafrenière *et al.* 2012), especially with regards to the partial rediploidization process which is still underway and not totally understood yet (Berthelot *et al.* 2014; Brieuc *et al.* 2014; Kodama *et al.* 2014; Sutherland *et*

al. 2016; Allendorf *et al.* 2015; Lien *et al.* 2016). A significantly improved understanding of this process has been achieved through increased efforts to map and compare chromosomal rearrangements among species (inversion, translocations, fissions and fusions), which helped to reconstruct the evolutionary history of salmonids genome architecture (Kodama *et al.* 2014; Sutherland *et al.* 2016). Furthermore, linkage mapping approaches have also improved the characterisation of the genomic regions that still exhibit tetrasomic inheritance patterns (Allendorf *et al.* 2015; Kodama *et al.* 2014; Lien *et al.* 2016; May and Delany 2015; Waples *et al.* 2016). The partial rediploidization of salmonid genomes is also known to challenge the development of genome-wide marker data sets. Indeed duplicated loci mostly located in tetrasomic regions (Allendorf *et al.* 2015) are usually underrepresent or even excluded in salmonid genomic studies (Hohenlohe *et al.* 2011; Hecht *et al.* 2012; Gagnaire *et al.* 2013b; Larson *et al.* 2014; Perrier *et al.* 2013; Leitwein *et al.* 2016)

The Eurasian brown trout (*Salmo trutta* L. 1758), is one of the most widespread freshwater species in the northern hemisphere, which presents high levels of phenotypic diversity linked to its complex evolutionary history (Elliott 1994; Bernatchez and Osinov 1995; Bernatchez, 2001). Natural brown trout populations have been intensely studied using molecular markers (Hansen *et al.* 2000; Sanz *et al.* 2006; Thaulow *et al.* 2014; Berrebi, 2015; Leitwein *et al.* 2016), but previous population genetics and phylogeography studies which usually relied on a limited number of markers did not integrate linkage map information (but see Hansen and Mensberg 2009; Hansen *et al.* 2010). The microsatellite linkage map available until now in brown trout (Gharbi *et al.* 2006) contains approximately 300 markers (288 microsatellites and 13 allozymes), which are distributed over 37 linkage groups (LGs) among the 40 LGs expected in this species (2*n*=80, Martinez *et al.* 1991; Philips and Ráb 2001). In order to follow the tendency towards an increasing number of markers in brown trout genetic studies (Leitwein *et al.* 2016), a higher density linkage map is needed to increase

mapping resolution and provide positional information for genome scans and association studies. The development of a high-density linkage map in brown trout should find at least two direct applications.

Although the brown trout is the closest relative of the Atlantic salmon (*S. salar* L. 1758), the two species drastically differ in their number of chromosomes (*S. salar* 2*n* = 54-58, Brenna-Hansen *et al.* [2012]; *S. trutta* 2*n* = 80, Philips and Ráb [2001]), indicative of a high frequency of chromosome rearrangements. For understanding the chromosomal evolution in the *Salmo* genus, a comparison between the genome architecture of the Atlantic salmon (Lien *et al.* 2016) and the brown trout, using other salmonid linkage maps as outgroups, is needed. The availability of important genomic resources in salmonids coupled with recent methodological advances in linkage maps comparison (Sutherland *et al.* 2016) provide favorable conditions to get new insights into the recent history of chromosomal rearrangement in the *Salmo* genus.

Another important application of a high-density linkage map in brown trout relates to understanding the consequences of human-mediated introductions of foreign and domestic genotypes in natural populations. The brown trout has been domesticated for decades, and wild populations have been heavily impacted by the stocking of genetically domesticated hatchery strains sometimes originating from distinct evolutionary lineages than the recipient populations (Elliot 1994; Laikre 1999; Berrebi *et al.* 2000; Bohling *et al.* 2016). These introductions have often resulted in the introgression of foreign alleles within wild brown trout populations, a generally negatively perceived phenomenon in conservation and management (Largiadèr and Scholl 1996; Poteaux *et al.* 1998, 1999; Hansen *et al.* 2000; Almodóvar *et al.* 2006; Sanz *et al.* 2006; Hansen and Mensberg 2009). However, the real evolutionary consequences of hybridization may take multiple facets (e.g., outbreeding depression, heterosis, adaptive introgression, decreased adaptive variation), the individual

effects of which remains largely unknown. In order to evaluate those potential fitness outcomes in brown trout, it would be necessary to combine the power of large SNP data sets (Leitwein *et al.* 2016) with a high-density linkage map and a detailed knowledge of chromosomal variation in recombination rate to perform comprehensive genome scans for introgression in natural populations.

The specific objectives of this study were: (i) to build a high-density linkage map in brown trout based on RAD markers developed by Leitwein *et al.* (2016) using reciprocal crosses of individuals belonging to two distinct evolutionary lineages (Atlantic and Mediterranean; Bernatchez, 2001); (ii) to characterize chromosome morphologies and centromere positions of metacentric chromosomes using the method recently developed in Limborg *et al.* (2015a); (iii) to perform map comparisons with the *S. salar* genome and an outgroup salmonid species to infer the timing of chromosome rearrangements during the recent evolutionary history of the *Salmo* genus, and (iv) to estimate the genome wide local variation in recombination rate and assess the consequence of this variation on the genomic landscape of nucleotide diversity in brown trout.

MATERIALS AND METHODS

Experimental crosses

Two F1 hybrid families, each comprising two parents and 150 offspring, were used for the linkage map analysis. Both were obtained by crossing one parent of Atlantic origin with one parent of Mediterranean origin *sensu* Bernatchez (2001). The F0 progenitors were either from a domestic Mediterranean strain lineage originally bred in the Babeau hatchery (described in Bohling *et al.* [2016]) and a domestic Atlantic strain lineage originating from the Cauterets

hatchery and independently reared from the Mediterranean strain at the Babeau hatchery. The Cauterets strain is one of the common, internationally-distributed Atlantic strains (comATL category; Bohling *et al.* 2016). Crosses were performed in December 2015 at the Babeau hatchery as follows: FAMILY 1: one Atlantic female × one Mediterranean male, and FAMILY 2: one Atlantic male × one Mediterranean female. Progenies were sacrificed in February 2016 after full resorption of the yolk sac (fish size ~ 2cm).

DNA extraction, library preparation and sequencing

Whole genomic DNA was extracted from caudal fin clips for the four parents of the two crosses and from tail clips for 150 offspring of each family using the commercial Thermo Scientific KingFisher Flex Cell and Tissue DNA kit. Individual DNA concentration was quantified using both NanoDrop ND-8000 spectrophotometer (Thermo Fisher Scientific) and Qubit 1.0 Fluorometer (Invitrogen, Thermo Fisher Scientific). Double digest RAD sequencing library preparation was performed following Leitwein *et al.* (2016). Briefly, DNA was digested with two restriction enzymes (*Eco*RI-HF and *Msp*I), the digested genomic DNA was then ligated to adapters and barcodes. Ligated samples with unique barcodes were pooled in equimolar proportions and cleanPCR beads (GC Biotech, The Netherlands) were used to select fragments size between 200 and 700 base pairs (bp). The size selected template was amplified by PCR and tagged with unique index specifically designed for Illumina sequencing (Peterson *et al.* 2012). For progenies, PCR products were pooled in equimolar ratios into 4 pools. Each pool was sequenced in a single Illumina Hiseq 2500 lane (i.e. 75 F1 progenies per lane), producing 125bp paired-end reads. The 4 parents were sequenced in a single Illumina lane in order to obtain a higher coverage depth.

Genotyping pipeline

Bioinformatic analyses followed the same procedure as in Leitwein *et al.* (2016). Briefly, raw reads passing Illumina purity filter and FastQC quality were demultiplexed, cleaned and trimmed with `process_radtags.pl` implemented in Stacks v1.35 (Catchen *et al.* 2013). The Atlantic salmon genome (GenBank accession number: GCA_000233375.4_ICSASG_v2) was used to determine individual genotypes at RAD markers using a reference mapping approach. First, reads were aligned to *S. salar* genome with the BWA-mem program (Li and Durbin, 2010). Alignment result files were processed into `pstacks` to build loci and call haplotypes for each individuals (using m = 3 and α = 0.05). Individuals with a minimum mean coverage depth under 7X were removed, resulting in a data set of 147 offspring in FAMILY 1 and 149 offspring in FAMILY 2. Hereafter, a RAD locus is defined as a sequence of 120bp, and thus can contain more than one SNP defining different haplotypes. A reference catalog of RAD loci was built with `cstacks` from the four parents of the two crosses (FAMILY 1 and FAMILY 2). Each individual offspring and each parent were then matched against the catalog with `sstacks`. Then, for each family independently, the module `genotypes` was executed to identify mappable makers that were genotyped in at least 130 offspring in each family, and with a minimum sequencing depth of 5 reads per allele. The correction option (-c) in the `genotypes` module was used for automated correction of false-negative heterozygote calls. The map type "cross CP" for heterogeneously heterozygous populations was selected to export haplotypic genotypes in the JoinMap 4.0 format (Van Ooijen, 2006). We only kept the loci shared between FAMILY 1 and FAMILY 2, for importation into JoinMap, leaving a total of 7680 mappable loci in both families.

Linkage mapping

198 Both family data sets were imported and filtered into JoinMap 4.0 (Van Ooijen, 2006) to
199 remove (i) loci presenting significant segregation distortion, (ii) loci in perfect linkage (i.e.,
200 similarity of loci = 1), and (iii) individuals with high rates of missing genotypes (>25%).
201 After this first filtering step, 5,635 and 5,031 loci remained in FAMILY 1 and FAMILY 2
202 respectively. Only those that were shared by the two families were kept, resulting in a subset
203 of 4,270 filtered informative loci. A random subset of 4,000 loci for both FAMILY 1 and
204 FAMILY 2 were reloaded into JoinMap 4.0 (i.e., the maximum number of loci handled by the
205 program). We then discarded 4 offspring in FAMILY 1 and 6 offspring in FAMILY 2 due to high
206 rates of missing genotypes (above 20%). Markers were then grouped independently within
207 each family using the "independence LOD" parameter in JoinMap 4.0 with a minimum LOD
208 value of 10. Unassigned markers were secondly assigned using the strongest cross-linkage
209 option with a LOD threshold of 5. Marker ordering was finally estimated within each group
210 using the regression mapping algorithm and three rounds of ordering. The Kosambi's
211 mapping function was used to estimate genetic distances between markers in centimorgans
212 (cM). Loci with undetermined linkage were then removed, and a consensus map was
213 produced between families using the map integration function after identifying homologous
214 LGs between FAMILY 1 and FAMILY 2.

215

216 **Estimation of centromere location and chromosome type**

217 The method recently developed by Limborg *et al.* (2015a) was used to identify chromosome
218 types (acrocentric, metacentric) and to determine the approximate centromere position of
219 metacentric chromosomes. This method uses phased progeny's genotypes to detect individual
220 recombination events by comparison to parental haplotype combinations. For each LG, the
221 cumulated number of recombination events between the first marker and increasingly distant
222 markers was computed from both extremities, using each terminal marker as a reference

starting point. We used the subset of markers that were found heterozygous only in the female parent to phase progeny's haplotypes within each family. We only focused on female informative sites because the lower recombination rate in male salmonids makes them less adequate for inferring centromere locations (Limborg *et al.* 2015a). Lower recombination in male brown trout was reported by Gharbi *et al.* (2006). The phased genotypes data sets were used to estimate recombination frequency (RFm) for intervals between markers along each LG. Finally, we plotted the RFm calculated from each LG extremity to determine the chromosome type and the approximate location of the centromere for metacentric chromosomes.

Map comparisons

The microsatellite linkage map established by Gharbi *et al.* (2006) was compared and anchored to our new high density linkage map using the MAPCOMP pipeline available at https://github.com/enormandeau/mapcomp/ (Sutherland *et al.* 2016). The microsatellite markers' primer sequences retrieved from Gharbi *et al.* (2006), as well as the five microsatellites used in Leitwein *et al.* (2016) and the lactate dehydrogenase (LDH-C1) gene from McMeel *et al.* (2001) were aligned with `BWA_aln` (Li and Durbin 2010) to the Atlantic salmon reference genome. Only single hit markers with a quality score (MAPQ) above 10 were retained. The 3,977 RAD markers integrated in the high density *S. trutta* linkage map (see results) were also aligned to the *S. salar* reference genome with `BWA_mem`. Microsatellite and LDH markers were anchored onto the RAD linkage map by identifying the closest RAD locus located on the same contig or scaffold. Pairing with closely linked RAD markers enabled us to position markers from the previous generation map onto the newly developed linkage map.

247

248 An additional comparison was performed between the *S. salar* high density linkage map
249 published by Tsai *et al.* (2016), and the *S. trutta* consensus linkage map developed in this
250 study. We used the alignment of Atlantic salmon and brown trout markers to the Atlantic
251 salmon reference genome obtained with `Bwa_mem` (Li and Durbin 2010) to identify loci
252 originating from orthologous genomic regions, and then used these loci in MAPCOMP
253 (Sutherland *et al.* 2016) to identify blocks of conserved synteny and orthologous chromosome
254 arms between the two species' maps. Conserved synteny blocks were visualized with the
255 web-based VGSC (Vector Graph toolkit of genome Synteny and Collinearity:
256 http://bio.njfu.edu.cn/vgsc-web/). The brook charr (*Salvelinus fontinalis*) linkage map
257 published in Sutherland *et al.* (2016) was used as one outgroup to provide orientation for
258 chromosome rearrangements during evolution of the *Salmo* lineage.

259 In order to estimate the genome-wide averaged net nucleotide divergence between *S. trutta*
260 and *S. salar* (d_a), we used the mean nucleotide diversity within *S. trutta* (π_w, averaged
261 between Atlantic and Mediterranean lineages) (Leitwein *et al.* 2016) and the absolute
262 nucleotide divergence between *S. trutta* and *S. salar* (π_b, also called d_{xy}). The net divergence
263 was estimated as $d_a = \pi_b - \pi_w$, by supposing that the mean nucleotide diversity in *S. salar*
264 (which is not available) was close to the mean nucleotide diversity estimated in *S. trutta*. To
265 estimate $\pi_{b,}$ we used the 3,977 consensus sequences of the RAD loci integrated in our *S. trutta*
266 linkage map, and aligned them with `BWA_mem` to the Atlantic salmon reference genome.
267 Then, the total number of mismatches divided by the total number of mapped nucleotides was
268 used to provide an estimate of π_b.

269

Estimation of genome-wide recombination rates

To estimate local variation in recombination rate across the genome, we compared our newly constructed genetic map of *S. trutta* to the physical map of *S. salar* with MAREYMAP (Rezvoy *et al*. 2007). In order to reconstruct a collinear reference genome for each brown trout linkage group, physical positions of brown trout RAD markers on the salmon genome were extracted from the `BWA_mem` alignment for each block of conserved synteny previously identified with MAPCOMP. The Loess method was used to estimate local recombination rates. It performs a local polynomial regression to fit the relationship between the physical and the genetic distances. The window size, defined as the percentage of the total number of markers to take into account for fitting the local polynomial curve, was set to 0.9 to account for local uncertainties due to the high rate of chromosomal rearrangements between species. A recombination rate equal to the weighted mean recombination rate of the two closest markers on the genetic map was assigned to the markers that were not used for fitting.

Correlation between recombination rate and nucleotide diversity

In order to test for a correlation between local recombination rate and nucleotide diversity in brown trout, we used the estimate of nucleotide diversity (π) in the Atlantic lineage (based on 20 individuals). These estimates of nucleotide diversity were taken from Leitwein *et al.* (2016), in which brown trout populations and hatchery strains of different origins showed highly correlated genome-wide variation patterns in nucleotide diversity. Markers with a recombination rate value above 2 cM/Mb or $\pi < 0.008$ were considered as outliers and were therefore removed from the analysis. This resulted in a dataset containing 3,038 markers for which both recombination rate and nucleotide diversity information were available.

Data availability

Table S1 contains the RAD markers IDs, the consensus sequences, the mapping position on the brown trout linkage map along with the position on the salmon genome and the estimation of the recombination rate. Figure S1 contains the RFm plots obtained for each female haploid data set. Table S2 contains the correspondence between the microsatellite and the new RAD linkage map. Figure S2 contains the MapComp figure comparing the Brown trout to the Atlantic salmon linkage map with markers paired through the Atlantic salmon genome.

RESULTS

Construction of a high-density linkage map in *Salmo trutta*

On average, 35M of filtered paired-end (PE) reads were obtained for each of the four parents (two families), and 5M PE reads for each of the 300 F1 (150 progenies per family) analyzed in this study. Therefore, the retained subset of 7,680 informative markers common to both families had a mean individual sequencing depth of 112X for the parents and 15X for the progenies, ensuring a good genotype calling quality in both families. Among these, a subset of 4,000 markers showing no segregation distortion in both families was randomly retained, to generate a consensus map between families 1 and 2. The resulting integrated map provides a sex- and lineage-averaged map, which is an important feature considering the reported differences in recombination rates between male and female in salmonids (Allendorf *et al.* 2015; Tsai *et al.* 2015), and the existence of divergent geographic lineages in brown trout (Bernatchez 2001).

A total of 3,977 markers were assigned to 40 *S. trutta* (*Str*) LGs on the integrated map (Figure 1), corresponding to the expected number of chromosomes in brown trout (Phillips and Ráb, 2001). The total map length was 1,403 cM, and individual LGs ranged from 14.6 cM (*Str*3; 47

318 markers) to 84.9 cM (*Str*37; 63 markers). The number of markers per LG ranged from 23 for
319 *Str*40 (15.2 cM) to 252 for *Str*1 (46.3 cM). Detailed information for each LG including the
320 density of markers per cM is reported in Table 1. Additional details concerning RAD markers
321 IDs, consensus sequences and mapping position on the salmon genome are reported in Table
322 S1.

323

324 **Location of centromeres and chromosome types**

325 The estimates of recombination frequencies obtained using the phased genotypes of female
326 progeny produced similar results for both FAMILY 1 and FAMILY 2. Individual linkage group
327 RFm plots obtained for each female haploid data set are provided in Figure S1. Two examples
328 of RFm plots obtained in FAMILY 1 are reported in Figure 2 for *Str*22 and *Str*28. Following
329 Limborg *et al.* (2015a), the pattern observed for *Str*22 typically reflects an acrocentric
330 chromosome type (paired straight lines; Figure 2a), whereas *Str*28 illustrates a metacentric
331 pattern (mirrored hockey stick shapes; Figure 2b) with the centromere approximately located
332 around 70cM. The total number of probable acrocentric chromosomes (Figure 1; type A, n =
333 32) largely exceeded the number of metacentric chromosomes (Figure 1; type M, n = 3). The
334 approximate position of the centromere was determined for each of the three metacentric LGs
335 (Figure 1; green boxes). The chromosome type remained undetermined for five LGs (Figure
336 1; type U) due to a low resolution of the RFm plots (Figure S1).

337

338 **Linkage map comparisons**

339 A total of 87 microsatellites markers (82/160 from Gharbi *et al*. [2006], 5/5 from Leitwein *et*
340 *al*. [2016] and the LDH locus [McMeel *et al.* 2001]) were successfully mapped to the Atlantic
341 salmon genome, and anchored to the new brown trout linkage map using their pairing with

342 RAD markers, following the method developed in Sutherland *et al.* (2016) (Figure 1; red
343 dots). The correspondence between the microsatellite and the new RAD linkage map is
344 provided in Table S2.

345 The identification of orthologous chromosomes arms between S. *trutta* (40LGs) and *S. salar*
346 (29LGs) revealed frequent chromosomal rearrangements between the two species (Figure 3,
347 Table 1). We found 15 one-to-one ortholog pairs (e.g., *Ssa*6-*Str*5, *Ssa*28-*Str*14; Figure 3,
348 Table 1), 12 cases where salmon chromosomes correspond to either 2 or 3 LG in the brown
349 trout (e.g., *Ssa*1, *Ssa*2; Figure 3), and only two cases where brown trout LGs correspond to
350 two salmon chromosomes (*Str*1 and *Str*15; Figure 3). Local inversions between *S. salar* and *S.*
351 *trutta* genomes were also observed as for instance *S. salar* LG6 and *S. trutta* LG5 (Figure S2).
352 Apart from these inter- and intra-chromosomal rearrangements, a strongly conserved synteny
353 was observed between the brown trout and the Atlantic salmon genomes.

354 Comparison with the brook charr linkage map revealed orthologous genomic regions with the
355 brown trout and the Atlantic salmon (Table 1), thus allowing for the identification of ancestral
356 and derived chromosomes structures in the *Salmo* genus. We found 8 chromosomal
357 rearrangements that occurred in the ancestral lineage of the *Salmo* genus before speciation
358 between *S. trutta* and *S. salar*, including 5 events of fusions (e.g., *Sfon*31-*Sfon*14, Table 1 and
359 2) and 3 events of fission (e.g., *Sfon*08; Table 1 and Figure 4). While no rearrangement was
360 detected in the *S. trutta* branch, the Atlantic salmon branch contained 13 events of fusion and
361 2 events of fission (Figure 4). Among these fusion events, note that *Str17* and *Str39* are
362 related to *Ssa15*, which was previously suspected to effectively be the result of a fusion
363 (Phillips *et al.* 2009), but which is also known to host *SdY*, the male-determining system of
364 the Atlantic salmon (Li *et al.* 2011) and most salmonids (Yano *et al.* 2013). As the
365 microsatellite locus *OmyRT5TUF* was consistently shown to be linked to the *SdY* locus in the
366 brown trout (Gharbi *et al.* 2006; Li *et al.* 2011), it may indicate that LG *Str39* could support

367 the male determining system of brown trout as the *OmyRT5TUF* locus was detected on this
368 LG (Table S2). This has to be investigated further.

369 We estimated the average net nucleotide divergence between *S. trutta* and *S. salar* to d_a =
370 0.0187 (with π_b= 0.0228, and π_w= 0.0041).

371

372 **Estimations of genome-wide and local recombination rates**

373 The brown trout genome-wide recombination rate averaged across the 3,721 markers
374 anchored on the Atlantic salmon reference genome (RAD markers mapped to ungrouped
375 scaffolds were discarded), was estimated at 0.88 ± 0.55 cM/Mb, and ranged from 0.21 cM/Mb
376 (LG27) to 4.10 (LG 37) across linkage groups (Table 1, Table S1). Chromosomal variation in
377 local recombination rate was observed for most chromosomes (e.g., LG *str*9 and LG *str*23,
378 Figure 5). A significant positive correlation between local recombination rate and population
379 nucleotide diversity was detected (R^2 = 0.058; *p*-value < 0.001; Figure 6).

380

381 DISCUSSION

382 This study describes the first high density linkage map in the brown trout *Salmo trutta*,
383 which extends the microsatellite linkage map already available in this species (Gharbi *et al.*
384 2006). The map covered 1,403 cM and encompasses 3,977 non-distorted markers distributed
385 across 40 linkage groups for which their centromere location was determined. Results showed
386 consistent chromosome number and morphologies compared to the species' karyotype
387 (2*n*=80, NF=100; Phillips and Ráb 2001). High resolution mapping (3.15 markers per cM)
388 was insured by the use of two mapping families each containing 150 offspring, and the
389 number of markers informative in both families was close to the limit over which saturation is

expected (i.e., 4,200 markers). The homogeneous distribution of makers across the genome, and the estimation of averaged recombination distances between both evolutionary lineages and sexes provide a highly valuable resource for future genomic, aquaculture, conservation and eco-evolutionary studies in brown trout. Beyond these general interests, this new linkage map also reveals strikingly different rates of chromosomal rearrangements that happened between the brown trout and the Atlantic salmon since their recent divergence.

A new-generation RAD linkage map in brown trout

Comparison between the newly developed linkage map and the previous microsatellite map was made possible by the integration of 82 microsatellite markers from the former generation map (Gharbi *et al.* 2006). This enabled us to identify the correspondence between homologous LGs from the two maps, and to detect cases of LG merging (8/40) and LG splitting (9/40) in the microsatellite map compared to the RAD linkage map. Consistent with the reported overrepresentation of acrocentric compared to metacentric chromosome found in the brook charr (i.e., 8 metacentric and 34 acrocentric [Sutherland *et al.* 2016]), we found three metacentric morphologies against 32 acrocentric. This represents a total number of chromosome arms ranging from 86 to 96, which is lower but quite close to the 96-104 interval previously estimated in *S. trutta* (Martinez *et al.* 1991; Phillips and Ráb 2001). Our assessment of chromosome type did not perfectly match the results from Gharbi *et al.* (2006), since the three metacentric chromosomes identified here were found to be either acrocentric or undetermined in their study. However, the metacentric chromosomes *Str*2 and *Str*5 identified here had more than a single matching LG in the former microsatellite map, which suggests that these homologs represent the two telomeric regions of a larger metacentric linkage group which has been reconstructed in our study. On the contrary, the three metacentric chromosomes identified in Gharbi *et al.* (2006) appeared to be acrocentric using the phase information available from our dataset. This could be the consequence of

pseudolinkage in the microsatellite map built using males of hybrid origin, in which the preferential pairing of conspecific homeologs followed by alternate disjunction may have generated an excess of non-parental gametes (Morrison 1970; Wright *et al.* 1983; Allendorf *et al.* 2015). In our study, the possible effect of pseudolinkage was avoided by using non-hybrid parents with a single lineage ancestry, thus possibly explaining the observed differences with the previous generation map.

Besides pseudolinkage, another broader consequence of past WGD in salmonids is the existence of duplicated loci that share the same alleles due to homeologous recombination in telomeric regions (Wright *et al.* 1983; Allendorf and Danzmann 1997; Allendorf *et al.* 2015). These residual tetrasomic regions challenge traditional linkage map reconstruction methods since duplicated loci (isoloci) tend to show Mendelian segregation distortion, and are therefore frequently excluded from linkage mapping analyses. Alternative approaches can be used to detect homeologous regions in experimental crosses (Lien *et al.* 2011; Brieuc *et al.* 2014; Waples *et al.* 2015). In brown trout, genome-wide patterns of RAD markers density and nucleotide diversity projected on the Atlantic salmon reference genome were also shown to provide indications about the location of duplicated regions (Leitwein et al 2016). Although our new RAD linkage map is based on non-distorted markers and therefore probably displays a reduced marker density in regions exhibiting tetrasomic inheritance, it does not completely exclude such regions. This is illustrated by the mapping of multiple RAD loci within the seven pairs of homeologs chromosome arms that retain residual tetrasomy in the Atlantic salmon genome (Lien *et al.* 2016) (Figure 3). Except for 3 of these 14 regions that received relatively few markers (*Ssa*3q, *Ssa*11qa, *Ssa*17qa on the salmon map; Figure 3), the remaining arms were well covered in our RAD linkage map, indicating that the filtering of non-Mendelian markers did not completely exclude the telomeric regions affected by homeologous crossovers. This feature of our RAD linkage map should insure a more even

recombination rate estimation between sexes (Lien *et al.* 2011), since the commonly observed lower recombination rate in males compared to females in salmonids could be partly due to a poor characterization of telomeric regions in mapping studies (Allendorf *et al.* 2015). Thus, our final sex-averaged linkage map should not be affected by the integration of recombinational information from male meiosis, while providing at the same time more relevant estimates of recombination distances for future eco-evolutionary studies.

Following the same idea, integrating maps between parents of different lineage origins (Atlantic and Mediterranean) allowed us to generate a consensus linkage map in which the potential differences in recombination rates between these two allopatric lineages are smoothened. This is important for future conservation genomic studies, considering the extensive human-mediated admixture between Atlantic and Mediterranean brown trout populations in southern Europe (Berrebi *et al.* 2000; Sanz *et al.* 2006; Thaulow *et al.* 2014; Berrebi, 2015).

The recent evolution of chromosomal rearrangements in the Salmo genus

Salmonids are still undergoing a rediploidization process since a WGD event that occurred around 60 Mya (Crête-Lafrenière *et al.* 2012; Near *et al.* 2012; Macqueen and Johnston 2014; Lien *et al.* 2016). This process, also described as functional diploidization by Ohno (1970), was accompanied by numerous chromosomal rearrangements within the salmonid family, making linkage maps of prime importance for studying the complex history of chromosomal evolution in salmonids (Sutherland *et al.* 2016). Several studies have pointed out a particularly high number of chromosome rearrangements in the lineage leading to the Atlantic salmon, involving mainly chromosome fusions that reduced the number of chromosomes to 29 in this species (Allendorf and Thorgaard 1984; Lien *et al.* 2016; Sutherland *et al.* 2016). However, the timing of these rearrangements remains largely unknown due to the lack of a closely related species in previous studies. Because *S. trutta* is

the most closely related species to *S. salar* among salmonids, the new brown trout RAD linkage map allowed for inferring the phylogenetic positions of the chromosome arm rearrangements that occurred within the *Salmo* genus. The ancestral state of *Salmo* chromosome structure was further resolved using the brook charr as an outgroup, as well as other salmonid species when necessary (Sutherland *et al.* 2016). This enabled us to identify 5 fusion events (e.g., *Sfon*31-*Sfon*14, Table 1) and 3 fission events (e.g., *Sfon*08a and b, Table1) that occurred before the Atlantic salmon/brown trout speciation. Thus, most fissions and fusion events observed in the Atlantic salmon genome (Sutherland *et al.* 2016), specifically occurred after the divergence between the two Salmo species. The net nucleotide divergence between *S. salar* and *S. trutta* was estimated to 1.87%, which indicates a recent divergence time between these two sister species (i.e., less than 5 My). This estimate of nucleotide divergence should be compared to the previously reported estimate by Bernatchez *et al.* (1992) that was approx. 6%. It also probably challenges the >10My divergence time between *S. salar* and *S. trutta* reported in Crête-Lafrenière *et al.* (2012), and this point should be investigated further. Whatever the timing of divergence, all of the inter-chromosomal rearrangements that occurred after the salmon/trout speciation happened in *S. salar*. Indeed, we did not observe any fusion/fission event within the *S. trutta* branch (Figure 4), whereas 15 rearrangements mostly involving fusions (13 fusions and 2 fissions) specifically occurred in the Atlantic salmon branch. These Robertsonian translocations explain the increased number of metacentric chromosomes in the Atlantic salmon compared to the brown trout, which were produced by the recent fusion of acrocentric chromosomes (*Ssa*1 to *Ssa*4; Figure 3 and Table 1). However, fusion events could also result in the formation of acrocentric chromosomes in the Atlantic salmon (e.g., *Ssa*15; Figure 3 and Table1), thus explaining the apparent loss of chromosomes arms (Allendorf and Thorgaard 1984). Finally, intra-chromosomic rearrangements also occurred along the *S. salar* branch, such as, e.g., the inversion detected

490 within *Ssa*6 and *Str*5 (Figure 3 and Figure S2). Altogether, these result support the previous
491 views that many chromosomal rearrangements have occurred within the *Salmo* lineage
492 (Allendorf and Thorgaard 1984; Sutherland *et al.* 2016), but demonstrate that most of them
493 recently happened in the Atlantic salmon branch while at the same time *S. trutta* has retained
494 a chromosomal architecture close to the ancestral salmonid form. The reasons for such a
495 contrasted evolution of chromosome structure between these two species remain to be
496 investigated. The fact that natural, viable hybrids occur between *Salmo* species (e.g., Jones,
497 1947; Garcia de Léaniz and Verspoor 1989) indicate that rearrangements have relatively poor
498 consequences during meiosis, and in early life phases.

499 .

500 *Recombination rate variation across the brown trout genome*

501 Despite extensive chromosomal rearrangements in the *S. salar* lineage, we could identify
502 highly conserved synteny blocks within orthologous chromosome arms to reconstitute local
503 alignments between the brown trout linkage map and the salmon physical map. One of our
504 main objectives was to use these comparisons between maps to estimate local recombination
505 rate variations along each linkage group in *S. trutta* (Figure 5). The average genome-wide
506 recombination rate was estimated at 0.88 cM/Mb, however, with strong heterogeneity being
507 found across the genome. High recombination rate regions were observed at extremities of
508 some LGs (e.g., *Str*9; Figure 5), and genomic regions associated with very low recombination
509 rates were also observed (e.g., *Str*23; Figure 5). In order to provide an indirect assessment of
510 this local recombination rate estimation, for future eco-evolutionary studies, we verified that
511 the frequently observed positive correlation between local recombination rate and nucleotide
512 diversity (Corbett-Detig *et al.* 2015) also occurs in brown trout. In a comparative study across
513 a wide range of species, Corbett-Detig *et al.* (2015) showed that the strength of this
514 correlation is highly variable among species, being generally stronger in species with large *vs*

small census population size. Although brown trout populations are usually considered to have relatively small census sizes (Jorde and Ryman 1996; Palm *et al.* 2003; Jensen *et al.* 2005; Serbezov *et al.* 2012), a significantly positive correlation was found between local recombination rate and nucleotide diversity using polymorphism data from the Atlantic lineage. Thus, recombination rate variation across the brown trout genome shapes the chromosomal landscape of neutral genetic diversity by modulating the efficiency of selection (both positive and negative) at linked neutral sites.

Variation in local recombination rate across genomic regions not only affects genome-wide variation patterns of polymorphism, but also has profound influence on a range of evolutionary mechanisms of prime importance for eco-evolutionary studies in brown trout. This recombination map should therefore have beneficial outcomes for our understanding of inbreeding depression, local adaptation, and the historical demography of natural populations (Rezvory *et al.* 2007; Dukić *et al.* 2016; Racimo *et al.* 2015). It will also be of precious help for understanding genome-wide introgression patterns in natural populations that have been restocked with individuals from a different lineage. Finally, a detailed picture of recombination rate variation in brown trout will help for choosing SNPs for the design of genotyping arrays in future association mapping experiments (e.g., Bourret *et al.* 2013; Houston *et al.* 2014).

Conclusion

A high density sex- and lineage-averaged consensus linkage map for *S. trutta* was developed and the chromosome type (acrocentric or metacentric) of most linkage groups was identified. Interspecies comparisons with the Atlantic salmon allowed identifying genomic regions of highly conserved synteny within chromosome arms and contribute towards a better understanding of recent genome evolution following speciation in the genus *Salmo*. A recent and strong acceleration in the rate of chromosomal rearrangements was detected in the *S.*

salar branch. These results should stimulate further research toward understanding the contrasted evolution of chromosome structure in sister species with less than 2% net nucleotide divergence. Recombination rate variation was found to influence genome-wide nucleotide diversity patterns in brown trout. These new genomic resources will provide important tools for future genome scans, QTL mapping and genome-wide association studies in brown trout. It also paves the way for a new generation of conservation genomics approaches that will look at the fitness consequences of introgression of foreign alleles into wild populations at the haplotype level.

ACKNOWLEDGEMENTS

Authors wish to thanks E. Ravel and people from the Fédération Départementale de la Pêche de l'Hérault (France) and of the Babeau hatchery for their help at several steps of this project. We would like to thanks Y. Anselmetti for his kind advice on bioinformatics computing. Many thanks to M. Limborg for his helpful scripts and advice in particular for the centromere location. We thanks B. Sutherland for his suggestions with MapComp. This project largely benefited from the Montpellier Bioinformatics Biodiversity cluster computing platform. Pre-sequencing steps necessary to the production of SNP data were performed at the Genotyping and Sequencing facility of the LabEx CeMEB (Centre Méditerranéen pour l'Environnement et la Biodiversité, Montpellier), and RAD sequencing performed at MGX (Montpellier GenomiX facility, Montpellier, France, http://www.mgx.cnrs.fr/). ML was partly supported by a grant of the LabEx CeMEB.

REFERENCES

563 Allendorf, F.W., S. Bassham, W.A. Cresko, M.T. Limborg, L.W. Seeb, and J.E. Seeb 2015
564 Effects of Crossovers Between Homeologs on Inheritance and Population Genomics
565 in Polyploid-Derived Salmonid Fishes. J Hered esv015.
566 Allendorf, F.W., and G.H. Thorgaard, 1984 Tetraploidy and the Evolution of Salmonid
567 Fishes, in: Turner, B.J. (Ed.), Evolutionary Genetics of Fishes, Monographs in
568 Evolutionary Biology. Springer US. 1: 1–53.
569 Almodóvar, A., G.G. Nicola, B. Elvira, and J.L. García-Marin, 2006 Introgression variability
570 among Iberian brown trout Evolutionary Significant Units: the influence of local
571 management and environmental features. Freshwater Biology 51: 1175–1187.
572 Amores, A., J. Catchen, A. Ferrara, Q. Fontenot, J.H Postlethwait, 2011 Genome Evolution
573 and Meiotic Maps by Massively Parallel DNA Sequencing: Spotted Gar, an Outgroup
574 for the Teleost Genome Duplication. Genetics 188: 799–808.
575 Bernatchez, L., 2001 The evolutionary history of brown trout (Salmo trutta L.) inferred from
576 phylogeographic, nested clade, and mismatch analyses of mitochondrial DNA
577 variation. Evolution 55: 351–379.
578 Bernatchez, L., R. Guyomard, and F. Bonhomme, 1992 DNA sequence variation of the
579 mitochondrial control region among geographically and morphologically remote
580 European brown trout Saltno trutta populations. Molecular Ecology 1: 161–173.
581 Bernatchez, L., and A. Osinov, 1995 Genetic diversity of trout (genus Salmo) from its most
582 eastern native range based on mitochondrial DNA and nuclear gene variation.
583 Molecular Ecology 4: 285–298.
584 Berrebi, P., 2015 Three brown trout Salmo trutta lineages in Corsica described through
585 allozyme variation. Journal of fish biology 86: 60–73.

586 Berrebi, P., C. Poteaux, M. Fissier, and G. Cattaneo-Berrebi, 2000 Stocking impact and
587 allozyme diversity in brown trout from Mediterranean southern France. Journal of
588 Fish Biology 56: 949–960.
589 Berthelot, C., F. Brunet, D. Chalopin, A. Juanchich, M. Bernard, *et al.*, 2014 The rainbow
590 trout genome provides novel insights into evolution after whole-genome duplication in
591 vertebrates. Nature communications 5.
592 Bohling, J., P. Haffray, and P. Berrebi, 2016 Genetic diversity and population structure of
593 domestic brown trout (Salmo trutta) in France. Aquaculture 462: 1–9.
594 Bourret, V., M.P. Kent, C.R. Primmer, A. Vasemägi, S. Karlsson, *et al.*, 2013 SNP-array
595 reveals genome-wide patterns of geographical and potential adaptive divergence
596 across the natural range of Atlantic salmon (Salmo salar). Molecular ecology 22: 532–
597 551.
598 Brieuc, M.S., C.D. Waters, J.E. Seeb, and K.A. Naish, 2014 A dense linkage map for Chinook
599 salmon (Oncorhynchus tshawytscha) reveals variable chromosomal divergence after
600 an ancestral whole genome duplication event. G3. 4: 447–460.
601 Catchen, J., P.A Hohenlohe, S. Bassham, A. Amores, and W.A Cresko, 2013 Stacks: an
602 analysis tool set for population genomics. Molecular ecology 22: 3124–3140.
603 Corbett-Detig, R.B., D.L. Hartl, and T.B. Sackton, 2015 Natural Selection Constrains Neutral
604 Diversity across A Wide Range of Species. PLOS Biol 13: e1002112.
605 Crête-Lafrenière, A., L.K. Weir, and L. Bernatchez, 2012 Framing the Salmonidae Family
606 Phylogenetic Portrait: A More Complete Picture from Increased Taxon Sampling.
607 PLOS ONE 7: e46662.
608 Dukić, M., D. Berner, M. Roesti, C.R. Haag, and D. Ebert, 2016 A high-density genetic map
609 reveals variation in recombination rate across the genome of Daphnia magna. BMC
610 Genetics 17: 137.

611 Ekblom, R., and J. Galindo, 2011 Applications of next generation sequencing in molecular
612 ecology of non-model organisms. Heredity 107: 1–15.
613 Elliott, J.M., 1994 Quantitative Ecology and the Brown Trout. Oxford University Press, USA.
614 Everett, M.V., M.R. Miller, and J.E. Seeb 2012 Meiotic maps of sockeye salmon derived from
615 massively parallel DNA sequencing. BMC Genomics 13: 521.
616 Gagnaire, P.-A., E. Normandeau, S.A. Pavey, and L. Bernatchez, 2013a Mapping phenotypic,
617 expression and transmission ratio distortion QTL using RAD markers in the Lake
618 Whitefish (Coregonus clupeaformis). Mol Ecol 22: 3036–3048.
619 Gagnaire, P.-A., S.A. Pavey, E. Normandeau, and L. Bernatchez, 2013b The Genetic
620 Architecture of Reproductive Isolation During Speciation-with-Gene-Flow in Lake
621 Whitefish Species Pairs Assessed by Rad Sequencing. Evolution 67: 2483–2497.
622 Garcia de Léaniz, C., and E. Verspoor, 1989 Natural hybridization between Atlantic salmon,
623 Salmo salar, and brown trout, Salmo trutta, in northern Spain. J. Fish Biol 34: 41–46.
624 Gharbi, K., A. Gautier, R.G. Danzmann, S. Gharbi, T. Sakamoto *et al.*, 2006 A linkage map
625 for brown trout (Salmo trutta): chromosome homeologies and comparative genome
626 organization with other salmonid fish. Genetics 172: 2405–2419.
627 Gonen, S., N.R. Lowe, T. Cezard, K. Gharbi, S.C. Bishop, *et al.*, 2014 Linkage maps of the
628 Atlantic salmon (Salmo salar) genome derived from RAD sequencing. BMC genomics
629 15: 1.
630 Hansen, M.M., K. Meier, and K.L.D Mensberg, 2010 Identifying footprints of selection in
631 stocked brown trout populations: a spatio-temporal approach. Molecular Ecology 19:
632 1787–1800.
633 Hansen, M.M., and K.L.D Mensberg, 2009 Admixture analysis of stocked brown trout
634 populations using mapped microsatellite DNA markers: indigenous trout persist in
635 introgressed populations. Biology Letters 5: 656–659.

636 Hansen, M.M., D.E. Ruzzante, E.E. Nielsen, and K.D. Mensberg, 2000 Microsatellite and
637 mitochondrial DNA polymorphism reveals life-history dependent interbreeding
638 between hatchery and wild brown trout (Salmo trutta L.). Molecular Ecology 9: 583–
639 594.
640 Hecht, B.C., F.P. Thrower, M.C. Hale, M.R. Miller, and K.M. Nichols, 2012 Genetic
641 Architecture of Migration-Related Traits in Rainbow and Steelhead Trout,
642 Oncorhynchus mykiss. G3. 2: 1113–1127.
643 Hohenlohe, P.A., S.J. Amish, J.M. Catchen, F.W. Allendorf, and G. Luikart, 2011 Next-
644 generation RAD sequencing identifies thousands of SNPs for assessing hybridization
645 between rainbow and westslope cutthroat trout. Molecular ecology resources 11: 117–
646 122.
647 Houston, R.D., J.W. Davey, S.C. Bishop, N.R. Lowe, J.C. Mota-Velasco, *et al*., 2012
648 Characterisation of QTL-linked and genome-wide restriction site-associated DNA
649 (RAD) markers in farmed Atlantic salmon. BMC Genomics 13: 244.
650 Houston, R.D., J.B. Taggart, T. Cézard, M. Bekaert, N.R. Lowe, *et al*., 2014 Development
651 and validation of a high density SNP genotyping array for Atlantic salmon (Salmo
652 salar). BMC genomics 15, 90.
653 Jensen, L.F., M.M. Hansen, J. Carlsson, V. Loeschcke, and K.L.D. Mensberg, 2005 Spatial
654 and temporal genetic differentiation and effective population size of brown trout
655 (Salmo trutta, L.) in small Danish rivers. Conserv Genet 6: 615–621.
656 Jones, J. w., 1947 Salmon and Trout Hybrids. Proceedings of the Zoological Society of
657 London 117: 708–715.
658 Jorde, P.E., and N. Ryman, 1996 Demographic Genetics of Brown Trout (Salmo trutta) and
659 Estimation of Effective Population Size From Temporal Change of Allele
660 Frequencies. Genetics 143: 1369–1381.

661 Kai, W., K. Nomura, A. Fujiwara, Y. Nakamura, M. Yasuike, *et al*., 2014 A ddRAD-based
662 genetic map and its integration with the genome assembly of Japanese eel (Anguilla
663 japonica) provides insights into genome evolution after the teleost-specific genome
664 duplication. BMC Genomics 15: 233.
665 Kodama, M., M.S.O Brieuc, R.H. Devlin, J.J. Hard, and K.A. Naish, 2014 Comparative
666 Mapping Between Coho Salmon (Oncorhynchus kisutch) and Three Other Salmonids
667 Suggests a Role for Chromosomal Rearrangements in the Retention of Duplicated
668 Regions Following a Whole Genome Duplication Event. G3 4: 1717–1730.
669 Kai, W., K. Nomura, A. Fujiwara, Y. Nakamura, M. Yasuike, *et al.*, 2014 A ddRAD-based
670 genetic map and its integration with the genome assembly of Japanese eel (Anguilla
671 japonica) provides insights into genome evolution after the teleost-specific genome
672 duplication. BMC Genomics 15: 233.
673 Kuang, Y.-Y., X.-H Zheng,. C.-Y. Li, X.-M Li, D.-C. Cao, *et al.*, 2016 The genetic map of
674 goldfish (Carassius auratus) provided insights to the divergent genome evolutions in
675 the Cyprinidae family. Scientific Reports 6.
676 Kumar, G., and M. Kocour, 2017 Applications of next-generation sequencing in fisheries
677 research: A review. Fisheries Research 186: 11–22.
678 Lamaze, F.C., C. Sauvage, A. Marie, D. Garant, and L. Bernatchez, 2012 Dynamics of
679 introgressive hybridization assessed by SNP population genomics of coding genes in
680 stocked brook charr (Salvelinus fontinalis). Molecular Ecology 21: 2877–2895.
681 Largiader, C.R., and A. Scholl, 1996 Genetic introgression between native and introduced
682 brown trout Salmo trutta L. populations in the Rhone River Basin. Molecular Ecology
683 5: 417–426.
684 Larson, W.A., G.J. McKinney, M.T. Limborg, M.V. Everett, M.V., L.W. Seeb, L.W *et al*.,
685 2016 Identification of Multiple QTL Hotspots in Sockeye Salmon (*Oncorhynchus*

686 *nerka*) Using Genotyping-by-Sequencing and a Dense Linkage Map. Journal of
687 Heredity 107: 122–133.
688 Larson, W.A., L.W. Seeb, M.V. Everett, R.K. Waples, W.D. Templin, *et al*., 2014
689 Genotyping by sequencing resolves shallow population structure to inform
690 conservation of Chinook salmon (Oncorhynchus tshawytscha). Evolutionary
691 Applications 7 : 355–369.
692 Leitwein, M., P.A. Gagnaire, E. Desmarais, S. Guendouz, M. Rohmer, *et al*., 2016 Genome-
693 wide nucleotide diversity of hatchery-reared Atlantic and Mediterranean strains of
694 brown trout Salmo trutta compared to wild Mediterranean populations. J. Fish. Biol.
695 89: 2717–2734.
696 Lien, S., B.F. Koop, S.R. Sandve, J.R. Miller, M.P. Kent, *et al*., 2016 The Atlantic salmon
697 genome provides insights into rediploidization. Nature 533: 200–205.
698 Li, H., and R. Durbin, 2010 Fast and accurate long-read alignment with Burrows–Wheeler
699 transform. Bioinformatics 26: 589–595.
700 Limborg, M.T., G.J. McKinney, L.W. Seeb, and J.E Seeb, 2015a. Recombination patterns
701 reveal information about centromere location on linkage maps. Mol. Ecol. Resour. 16:
702 655–661.
703 Limborg, M.T., Waples, R.K., Allendorf, F.W., Seeb, J.E., 2015b Linkage Mapping Reveals
704 Strong Chiasma Interference in Sockeye Salmon: Implications for Interpreting
705 Genomic Data. G3. 5: 2463–2473.
706 Limborg, M.T., Waples, R.K., Seeb, J.E., Seeb, L.W., 2014. Temporally Isolated Lineages of
707 Pink Salmon Reveal Unique Signatures of Selection on Distinct Pools of Standing
708 Genetic Variation. J. Hered. esu063.

709 Liu, S., Y. Li, Z. Qin, X. Geng, L. Bao, *et al*., 2016 High-density interspecific genetic linkage
710 mapping provides insights into genomic incompatibility between channel catfish and
711 blue catfish. Animal genetics 47: 81–90.
712 Macqueen, D.J., and I.A. Johnston, 2014 A well-constrained estimate for the timing of the
713 salmonid whole genome duplication reveals major decoupling from species
714 diversification. Proceedings of the Royal Society of London B: Biological Sciences
715 281: 20132881.
716 Martinez, P., A. Vinas, C. Bouza, J. Arias, R. Amaro, *et al*.,1991 Cytogenetical
717 characterization of hatchery stocks and natural populations of sea and brown trout
718 from northwestern Spain. Heredity 66: 9–17.
719 May, B., and M.E. Delany, 2015 Meiotic Models to Explain Classical Linkage,
720 Pseudolinkage, and Chromosomal Pairing in Tetraploid Derivative Salmonid
721 Genomes: II. Wright is Still Right. J Hered 106: 762–766.
722 McKinney, G., L. Seeb, W. Larson, D. Gomez-Uchida, M. Limborg, M., *et al*., 2015 An
723 integrated linkage map reveals candidate genes underlying adaptive variation in
724 Chinook salmon (*Oncorhynchus tshawytscha*). Mol Ecol Resour 16: 769–783.
725 McMeel, O.M., E.M. Hoey, and A. Ferguson, 2001 Partial nucleotide sequences, and routine
726 typing by polymerase chain reaction–restriction fragment length polymorphism, of the
727 brown trout (*Salmo trutta*) lactate dehydrogenase, LDH-C1*90 and *100 alleles.
728 Molecular Ecology 10: 29–34.
729 Morrison, W.J., 1970 Nonrandom segregation of two lactate dehydrogenase subunit loci in
730 trout. Transactions of the American Fisheries Society 99: 193–206.
731 Near, T.J., R.I. Eytan, A. Dornburg, K.L. Kuhn, J.A. Moore, *et al*., 2012 Resolution of ray-
732 finned fish phylogeny and timing of diversification. PNAS 109: 13698–13703.

733 Ohno, S., 1970 The Enormous Diversity in Genome Sizes of Fish as a Reflection of Nature's
734 Extensive Experiments with Gene Duplication. Transactions of the American
735 Fisheries Society 99: 120–130.
736 Palm, S., L. Laikre, P.E. Jorde, and N. Ryman, 2003 Effective population size and temporal
737 genetic change in stream resident brown trout (*Salmo trutta, L.*). Conservation
738 Genetics 4: 249–264.
739 Perrier, C., V. Bourret, M.P. Kent, and L. Bernatchez, 2013 Parallel and nonparallel genome-
740 wide divergence among replicate population pairs of freshwater and anadromous
741 Atlantic salmon. Molecular Ecology 22: 5577–5593.
742 Peterson, B.K., J.N. Weber, E.H. Kay, H.S. Fisher, and H.E. Hoekstra, 2012 Double digest
743 RADseq: an inexpensive method for de novo SNP discovery and genotyping in model
744 and non-model species. PloS one 7: e37135.
745 Phillips, R.B., K.A. Keatley, M.R. Morasch, A.B. Ventura, K.P. Lubieniecki, *et al.*, 2009
746 Assignment of Atlantic salmon (*Salmo salar*) linkage groups to specific
747 chromosomes: conservation of large syntenic blocks corresponding to whole
748 chromosome arms in rainbow trout (*Oncorhynchus mykiss*). Bmc Genetics 10: 1.
749 Phillips, R., and P. Ráb, 2001 Chromosome evolution in the Salmonidae (Pisces): an update.
750 Biological Reviews of the Cambridge Philosophical Society 76: 1–25.
751 Poteaux, C., D. Beaudou, and P. Berrebi, 1998 Temporal variations of genetic introgression in
752 stocked brown trout populations. Journal of Fish Biology 53: 701–713.
753 Poteaux, C., F. Bonhomme, and P. Berrebi, 1999 Microsatellite polymorphism and genetic
754 impact of restocking in Mediterranean brown trout (*Salmo trutta L.*). Heredity 82:
755 645–653.
756 Racimo, F., S. Sankararaman, R. Nielsen, and E. Huerta-Sánchez, 2015. Evidence for archaic
757 adaptive introgression in humans. Nat Rev Genet 16, 359–371. doi:10.1038/nrg3936

758 Rezvoy, C., D. Charif, L. Guéguen, and G.A. Marais, 2007 MareyMap: an R-based tool with
759 graphical interface for estimating recombination rates. Bioinformatics 23: 2188–2189.
760 Rondeau, E.B., D.R. Minkley, J.S. Leong, A.M. Messmer, J.R. Jantzen, *et al.*, 2014 The
761 Genome and Linkage Map of the Northern Pike (Esox lucius): Conserved Synteny
762 Revealed between the Salmonid Sister Group and the Neoteleostei. PLOS ONE 9:
763 e102089.
764 Sanz, N., M. Cortey, C. Pla, and J.L. García-Marín, 2006 Hatchery introgression blurs ancient
765 hybridization between brown trout (*Salmo trutta*) lineages as indicated by
766 complementary allozymes and mtDNA markers. Biological Conservation 130: 278–
767 289.
768 Sauvage, C., M. Vagner, N. Derôme, C. Audet, and L. Bernatchez, 2012 Coding gene single
769 nucleotide polymorphism mapping and quantitative trait loci detection for
770 physiological reproductive traits in brook charr, *Salvelinus fontinalis*. G3: 2: 379–392.
771 Serbezov, D., P.E. Jorde, L. Bernatchez, E.M. Olsen, and L.A. Vøllestad, 2012 Life history
772 and demographic determinants of effective/census size ratios as exemplified by brown
773 trout (*Salmo trutta*). Evolutionary Applications 5: 607–618.
774 Slate, J., J. Gratten, D. Beraldi, J. Stapley, M. Hale, *et al.*, 2008 Gene mapping in the wild
775 with SNPs: guidelines and future directions. Genetica 136: 97–107.
776 Stapley, J., J. Reger, P.G.D. Feulner, C. Smadja, J. Galindo, *et al.*, 2010 Adaptation
777 genomics: the next generation. Trends in Ecology & Evolution 25: 705–712.
778 Sutherland, B.J.G., T. Gosselin, E. Normandeau, M. Lamothe, N. Isabel, *et al.*, 2016
779 Salmonid chromosome evolution as revealed by a novel method for comparing
780 RADseq linkage maps. Genome Biol Evol evw262. doi:10.1093/gbe/evw262

781 Thaulow, J., R. Borgstrøm, and M. Heun, 2014 Genetic persistence of an initially introduced
782 brown trout (*Salmo trutta L.*) population despite restocking of foreign conspecifics.
783 Ecol Freshw Fish 23: 485–497.
784 Tsai, H.Y., A. Hamilton, D.R. Guy, A.E. Tinch, S.C. Bishop, *et al.*, 2015 The genetic
785 architecture of growth and fillet traits in farmed Atlantic salmon (*Salmo salar*). Bmc
786 Genetics 16: 51.
787 Tsai, H.Y., D. Robledo, N.R. Lowe, M. Bekaert, J.B. Taggart, *et al.*, 2016 Construction and
788 Annotation of a High Density SNP Linkage Map of the Atlantic Salmon (*Salmo salar*)
789 Genome. G3. 6: 2173–2179.
790 Van Ooijen, J.W., 2006 JoinMap 4; Software for the calculation of genetic map in
791 experimental populations. Kyazma B.V., Wageningen, Netherlands.
792 Wang, L., Z.Y. Wan, B. Bai, S.Q. Huang, E. Chua, *et al.*, 2015 Construction of a high-density
793 linkage map and fine mapping of QTL for growth in Asian seabass. Sci. Rep. 5.
794 Waples, R.K., L.W. Seeb, and J.E. Seeb, 2016 Linkage mapping with paralogs exposes
795 regions of residual tetrasomic inheritance in chum salmon (*Oncorhynchus keta*). Mol.
796 Ecol. Res. 16: 17–28.
797 Wright Jr, J.E., K. Johnson, A. Hollister, B. May, 1983 Meiotic models to explain classical
798 linkage, pseudolinkage, and chromosome pairing in tetraploid derivative salmonid
799 genomes. Isozymes 10: 239–260.
800 Yano, A., B. Nicol, E. Jouanno, E. Quillet, A. Fostier, *et al.*, 2013 The sexually dimorphic on
801 the Y-chromosome gene (sdY) is a conserved male-specific Y-chromosome sequence
802 in many salmonids. Evolutionary applications 6: 486–496.
803 Zhao, L., Y. Zhang, P. Ji, X. Zhang, Z. Zhao, *et al.*, 2013 A Dense Genetic Linkage Map for
804 Common Carp and Its Integration with a BAC-Based Physical Map. PLOS ONE 8:
805 e63928

Table 1: Summary of the main features of the brown trout high density linkage map based on the 3,977 mapped markers, including correspondence with the former generation linkage map established by Gharbi et al. (2006). The mean recombination rate is reported for each LG, as well as syntenic relationships with homologous chromosome arms from Atlantic salmon and brook charr. Grey-shaded arms correspond to the seven pairs involved in homeologous pairing (i.e. tetrasomic inheritance) in *S. salar* (Lien et al. 2016).

LG	Distance (cM)	Number of SNP markers mapped to ech LG	density (markers/cM)	Recombination rate (cM/Mb)	Microsatellite LG_Map Gharbi et al. (2006)	Atlantic Salmon	Brook Charr
Str 1	46.308	252	5.44	1.43	BT-10	Ssa 16qb	Sfon 05a
					BT-06	Ssa 29	Sfon 05b
Str 2	45.621	130	2.85	0.82	BT-05	Ssa 7q	Sfon 02b
					BT-15	Ssa 7p	Sfon 02a
Str 3	14.635	47	3.21	0.39	BT-16 BT-24	Ssa 3q	Sfon 08a
Str 4	20.902	249	11.91	0.4	BT-32	Ssa 20qa	Sfon 40
Str 5	40.51	140	3.46	0.56	BT-6	Ssa 6q	Sfon 31
					BT-35	Ssa 6p	Sfon 14
Str 6	53.049	139	2.62	0.48	BT-27	Ssa 12qa	Sfon 03b
						Ssa 12qb	Sfon 03a
Str 7	28.088	102	3.63	0.7	BT-9	Ssa 25	Sfon 24
Str 8	19.814	96	4.85	0.89	-	Ssa 17qa	Sfon 39
Str 9	44.687	88	1.97	1.18	BT-13	Ssa 1p	Sfon 12
Str 10	32.513	85	2.61	0.68	BT-27	Ssa 13qb	Sfon 08b
Str 11	65.086	79	1.21	1.65	BT-12	Ssa 5q	Sfon 07a
						Ssa 5p	Sfon 07b
Str 12	33.021	60	1.82	0.7	-	Ssa 2p	Sfon 29
Str 13	28.807	64	2.22	0.36	-	Ssa 26	Sfon 06a
Str 14	47.143	61	1.29	1.23	BT-36	Ssa 28	Sfon 27
Str 15	29.805	59	1.98	1.6	BT-04	Ssa 4p	Sfon04b
						Ssa 23	Sfon 04a
Str 16	29.837	56	1.88	0.59	-	Ssa 1qb	Sfon 13
Str 17	40.655	24	0.59	1.13	BT-28	Ssa 15qb	Sfon 30
Str 18	25.58	207	8.09	0.5	BT-16	Ssa 3p	Sfon 11
Str 19	34.485	69	2	1.04	BT-22	Ssa 24	Sfon 06b
Str 20	23.814	60	2.52	0.65	-	Ssa 2q	Sfon 42
Str 21	42.194	187	4.43	1.43	BT-25	Ssa 16qa	Sfon 20
Str 22	30.433	145	4.76	0.6	BT-30	Ssa 4q	Sfon 09
Str 23	38.057	141	3.7	0.5	BT-02	Ssa 9qb	Sfon 33
						Ssa 9qc	Sfon 38
Str 24	37.805	139	3.68	1.11	BT-31	Ssa 21	Sfon 26
Str 25	23.843	131	5.49	0.63	BT-07	Ssa 10qb	Sfon 15
Str 26	41.025	113	2.75	0.45	BT-33	Ssa 22	Sfon 21
Str 27	33.275	111	3.34	0.21	BT-26	Ssa 13qa	Sfon 18
Str 28	35.425	109	3.08	1.05	BT-23	Ssa 18qa	Sfon 36

						Ssa 18qb	Sfon32
Str 29	36.675	105	2.86	0.52	BT-29	Ssa 27	Sfon 23
Str 30	21.4	102	4.77	0.37	BT-23	Ssa 1qa	Sfon 01b
Str 31	24	99	4.13	1.33	BT-02	Ssa 9qa	Sfon 35
Str 32	39.782	87	2.19	0.81	-	Ssa 14qa	Sfon 22
Str 33	20.438	73	3.57	1.23	-	Ssa 8q	Sfon 41
Str 34	31.085	67	2.16	1.03	BT-14	Ssa 20qb	Sfon 25
Str 35	44.948	68	1.51	1.22	BT-12 BT-35	Ssa 10qa	Sfon 17
Str 36	42.241	61	1.44	0.44	BT-13	Ssa 11qa Ssa 11qb	Sfon28 Sfon 10
Str 37	84.844	63	0.74	4.1	-	Ssa 14qb	Sfon34
Str 38	19.365	49	2.53	1.57	BT-15	Ssa 17qb	Sfon 37
Str 39	36.825	37	1	1.08	BT-28	Ssa 15qa	Sfon 19
Str 40	15.12	23	1.52	0.58	-	Ssa 19qb Ssa 19qa	Sfon 01a Sfon 16
Whole genome	**1403.14**	**3977**	**3.15**	**0.88**			

Legends of the figures:

Fig. 1. The brown trout (*Salmo trutta*) high density linkage map. Horizontal black lines within each of the 40 LGs represent mapped RAD markers (n = 3,977). The most probable chromosome type determined with the RFm method (Limborg et al. 2015a) is indicated above each LG (A: acrocentric, M: metacentric, U: undetermined). Green boxes indicate the approximate position of the centromere for metacentric LGs. Red dots represent the position of 89 additional markers that were transferred from the previous generation linkage map (see Table S2 for details).

Fig. 2. Plots illustrating the recombination frequency estimates (RFm) for intervals between markers along two different LGs. For each LG, RFm was calculated from both chromosomal extremities (right: red circles; left: blue circles), using each of the two terminal markers as a reference starting point. The RFm plot of (A) LG *str*22 illustrates a classical acrocentric pattern, while (B) LG *str*28 displays a classical metacentric pattern with a centromere position around 70 cM. The RFm plots of all brown trout LGs obtained in the two families are illustrated in Figure S1.

Fig. 3. Dual synteny plot showing conserved syntenic blocks and chromosome rearrangements between *Salmo salar* (*Ssa*) and *Salmo trutta* (*Str*) LGs. Chromosomes arms (p, q_a and q_b) are specified for *S. salar* LGs, and the seven pairs of chromosome arms that still exhibit residual tetrasomy in salmon appear in red (Lien et al., 2016).

Fig. 4: Summary of fission and fusion events within the *Salmo* genus, that were oriented using the brook charr (*Salvelinus fontinalis*) as an outgroup species. Rearrangements are classified with regards to their occurrence (a) before the *S. salar*/*S. trutta* speciation, (b) in the *S. salar* branch after speciation, or (c) in the *S. trutta* branch after speciation.

Fig. 5. Estimates of local recombination rate (ρ) in cM/Mb for markers located along two *Salmo trutta* linkage groups: (A) LG *Str*9 and (B) LG *Str*23. The average recombination rate (mean ρ) for each LG is given at the top left side of each figure. Local recombination rate estimates for other *S. trutta* LGs are reported in Table S1 and the average recombination rate of each LG is provided in Table 1.

Fig. 6. Genome-wide positive correlation between the mean nucleotide diversity in the Atlantic brown trout lineage (π) and the local recombination rate (ρ, in cM/Mb), based on 3,038 SNP markers (R^2 = 0.058; p-value <0.001).

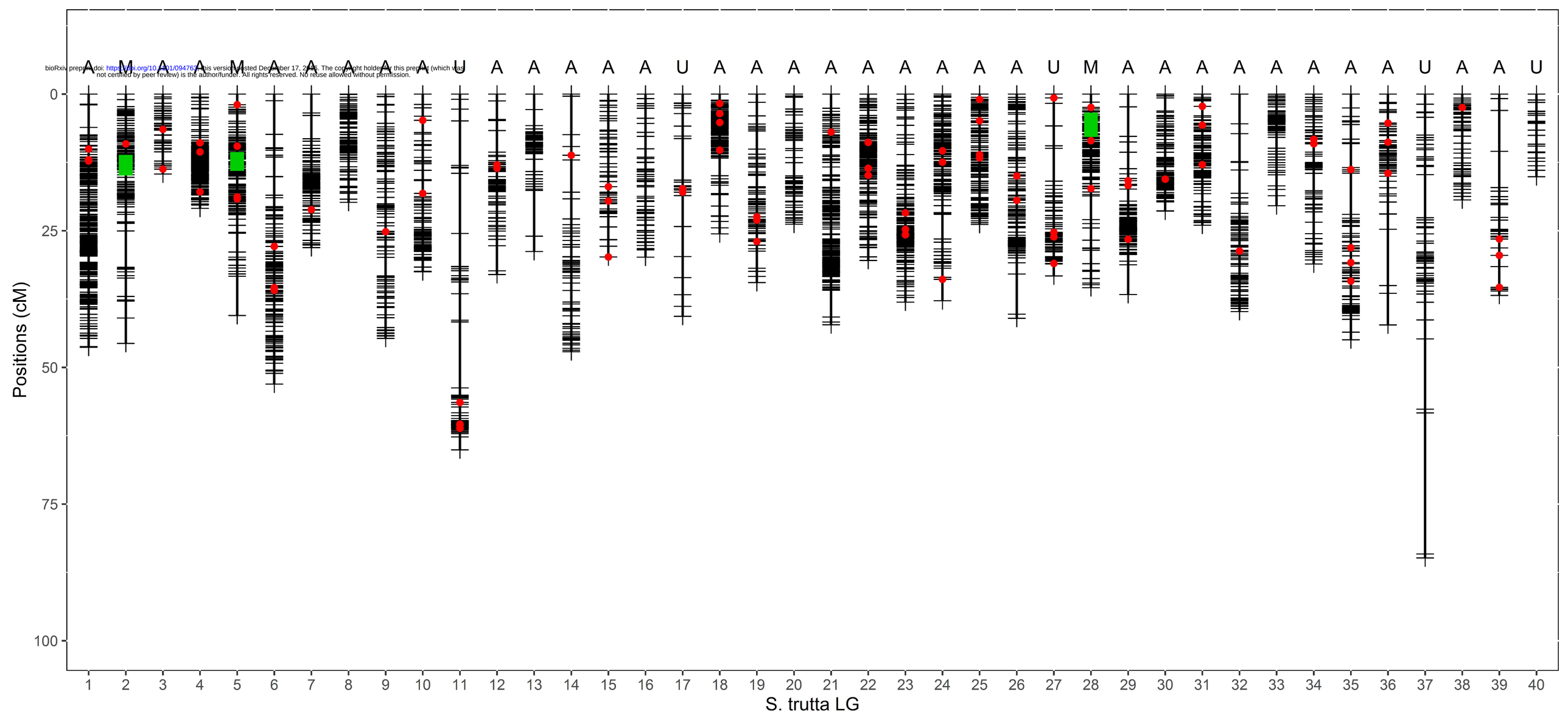

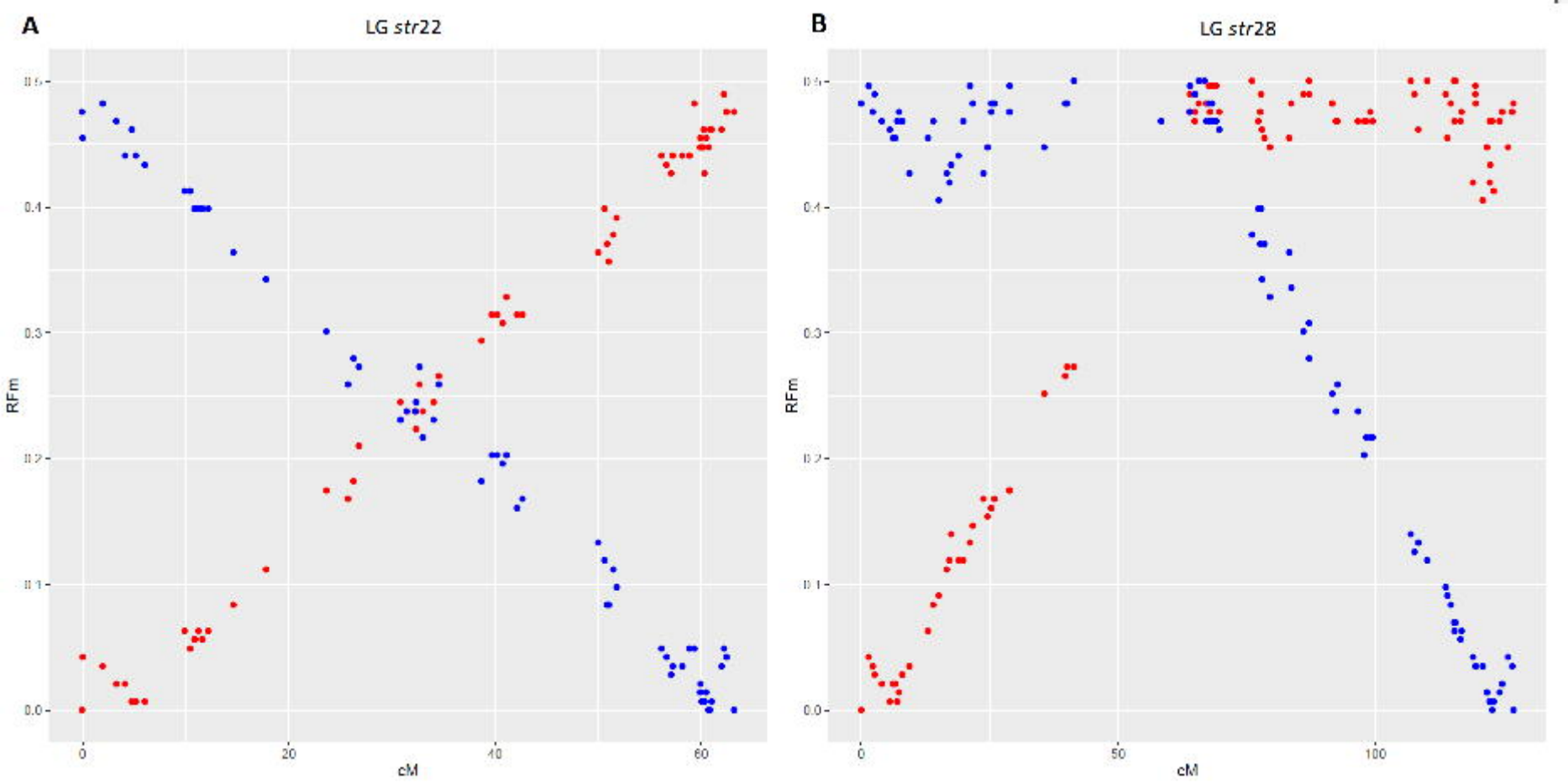
A
LG str22
RFm
cM
0.0
0.1
0.2
0.3
0.4
0.5
0
20
40
60
B
LG str28
RFm
cM
0.0
0.1
0.2
0.3
0.4
0.5
0
50
100

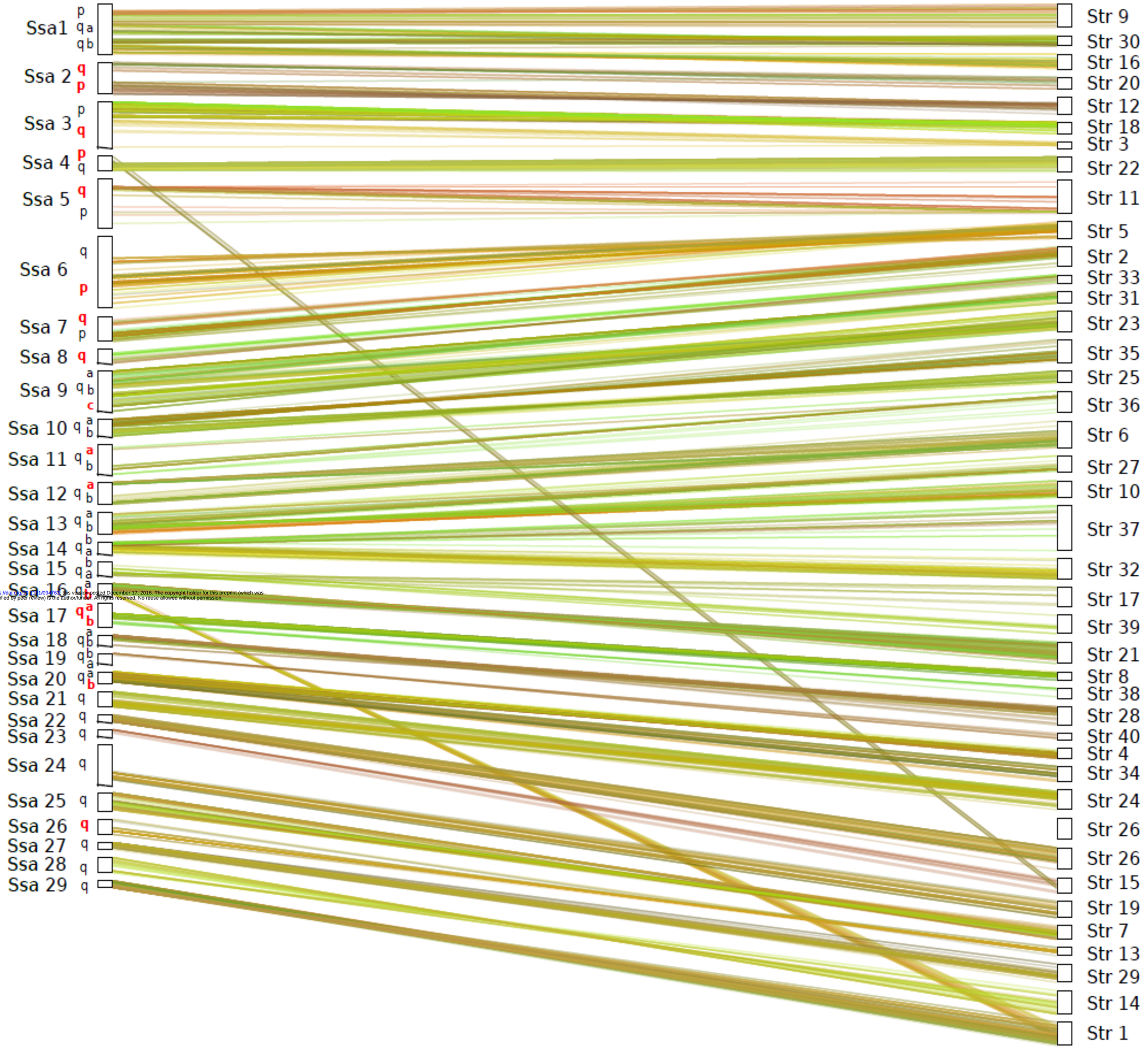

		Fusion	Fission
a	Salmo before speciation	5	3
b	*S. salar* after speciation	13	2
c	*S. trutta* after speciation	0	0

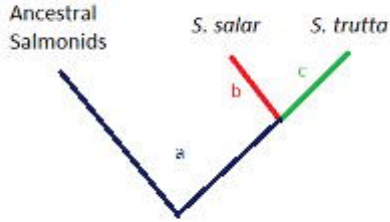

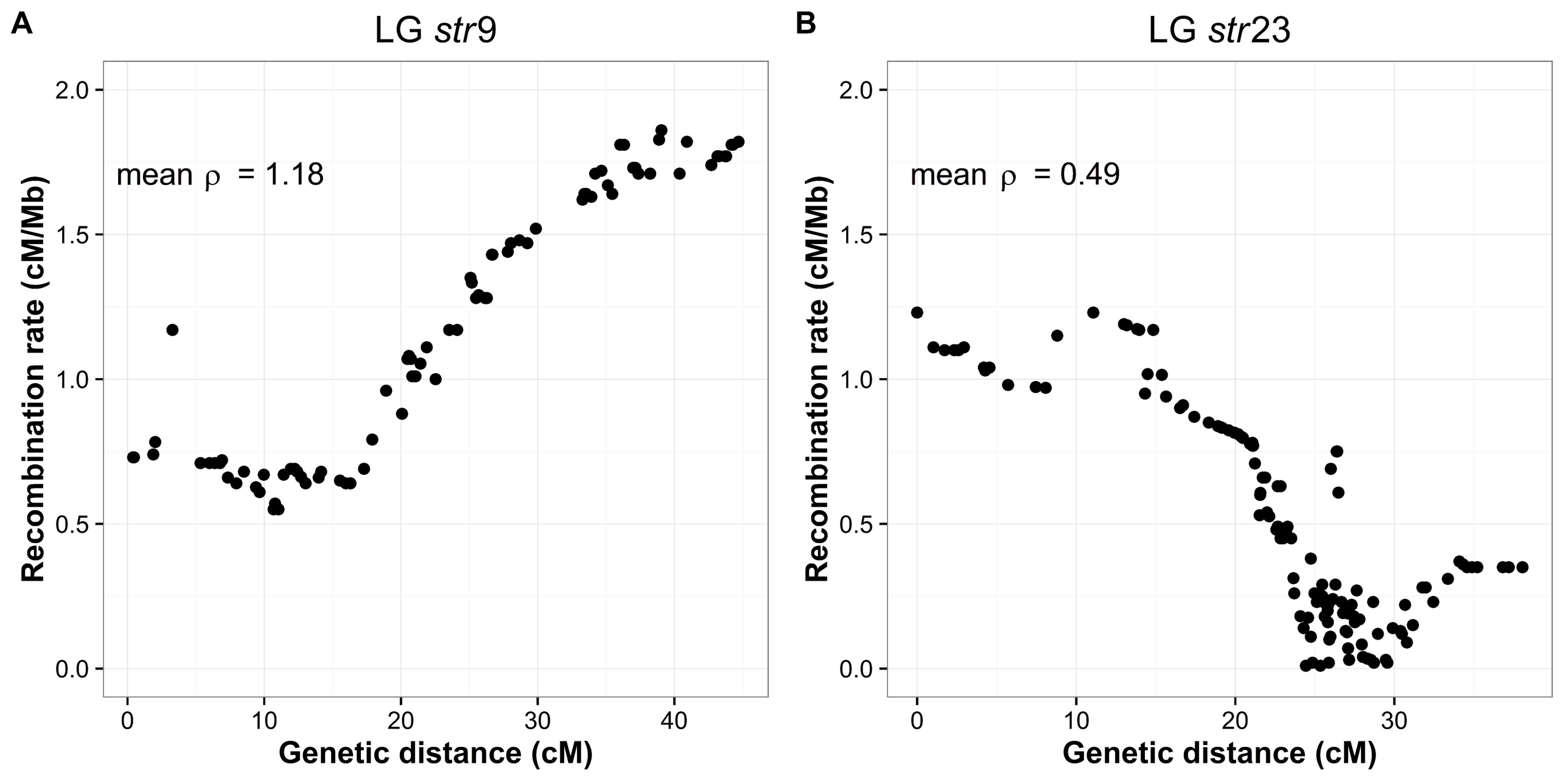
A
LG str9
mean ρ = 1.18
Recombination rate (cM/Mb)
Genetic distance (cM)
0.0
0.5
1.0
1.5
2.0
0
10
20
30
40
B
LG str23
mean ρ = 0.49
Recombination rate (cM/Mb)
Genetic distance (cM)
0.0
0.5
1.0
1.5
2.0
0
10
20
30

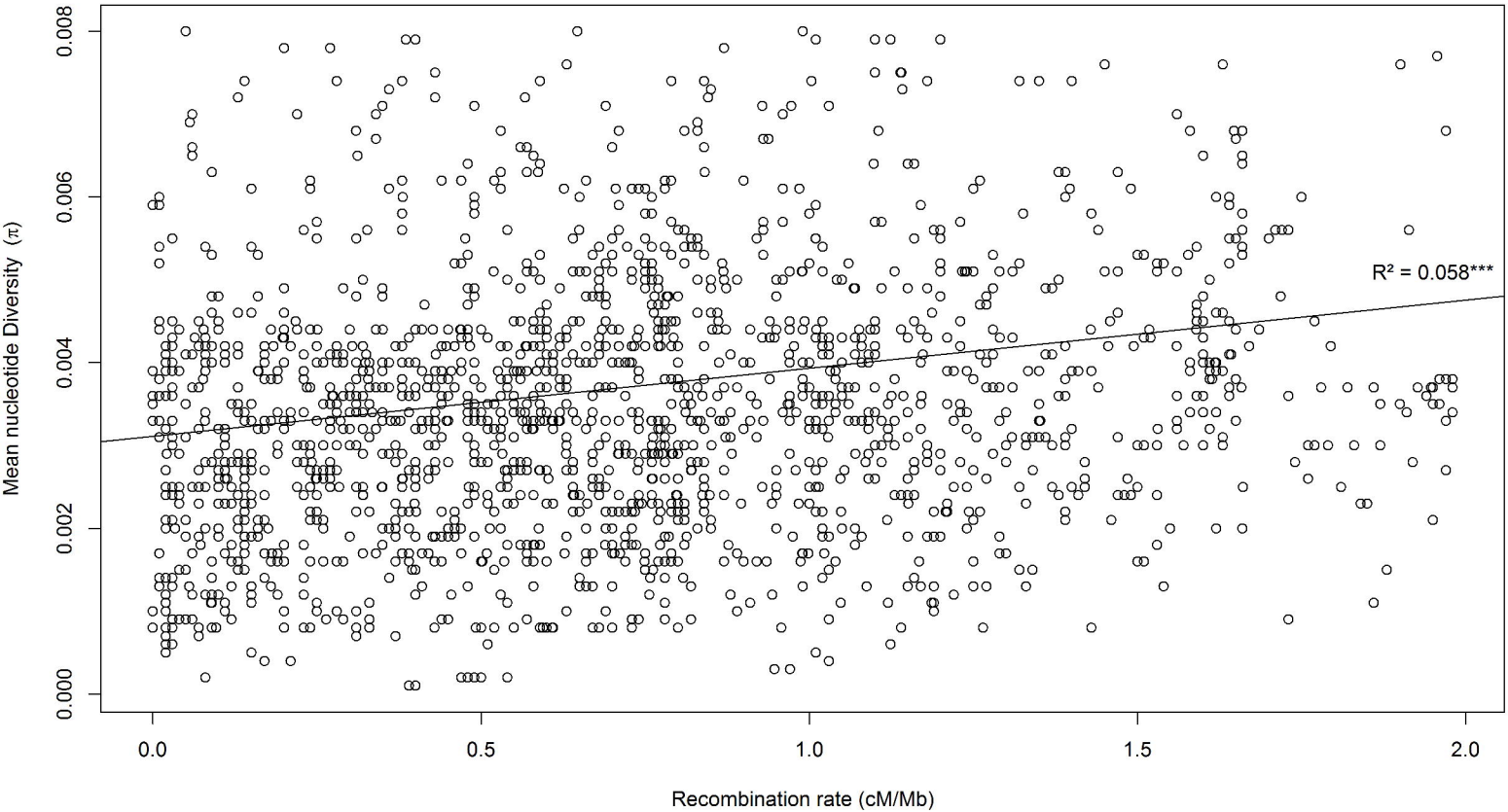
Mean nucleotide Diversity (π)
0.000
0.002
0.004
0.006
0.008
R² = 0.058***
0.0
0.5
1.0
1.5
2.0
Recombination rate (cM/Mb)